Biochimica et Biophysica Acta 1857 (2016) 1541–1549

Contents lists available at ScienceDirect

Biochimica et Biophysica Acta

journal homepage: www.elsevier.com/locate/bbabio

Effect of ionic strength on intra-protein electron transfer reactions: The case study of charge recombination within the bacterial reaction center

Mauro Giustini [a,b,*], Matteo Parente [c], Antonia Mallardi [d], Gerardo Palazzo [e,b,**]

[a] Chemistry Department, University of Rome "La Sapienza", Italy
[b] CSGI (Center for Colloid and Surface Science), c/o Dept. Chemistry, via Orabona 4, 70125 Bari, Italy
[c] Dutch Institute for Fundamental Energy Research (DIFFER), De Zaale 20, 5612, AJ, Eindhoven, The Netherlands
[d] CNR-IPCF, Istituto per i processi chimico fisici, c/o Dept. Chemistry, via Orabona 4, 70125 Bari, Italy
[e] Chemistry Department, University of Bari, via Orabona 4, 70125 Bari, Italy

ARTICLE INFO

Article history:
Received 25 April 2016
Received in revised form 6 June 2016
Accepted 9 June 2016
Available online 11 June 2016

Keywords:
Intra-protein electron transfer
Rhodobacter sphaeroides
Charge recombination
Hofmeister series, Debye screening length

ABSTRACT

It is a common believe that intra-protein electron transfer (ET) involving reactants and products that are overall electroneutral are not influenced by the ions of the surrounding solution. The results presented here show an electrostatic coupling between the ionic atmosphere surrounding a membrane protein (the reaction center (RC) from the photosynthetic bacterium *Rhodobacter sphaeroides*) and two very different intra-protein ET processes taking place within it. Specifically we have studied the effect of salt concentration on: i) the *kinetics* of the charge recombination between the reduced primary quinone acceptor Q_A^- and the primary photoxidized donor P^+; ii) the *thermodynamic equilibrium* ($Q_A^- \leftrightarrow Q_B^-$) for the ET between Q_A^- and the secondary quinone acceptor Q_B. A distinctive point of this investigation is that reactants and products are overall electroneutral. The protein electrostatics has been described adopting the lowest level of complexity sufficient to grasp the experimental phenomenology and the impact of salt on the relative free energy level of reactants and products has been evaluated according to suitable thermodynamic cycles. The ionic strength effect was found to be independent on the ion nature for $P^+Q_A^-$ charge recombination where the leading electrostatic term was the dipole moment. In the case of the $Q_A^- \leftrightarrow Q_B^-$ equilibrium, the relative stability of Q_A^- and Q_B^- was found to depend on the salt concentration in a fashion that is different for chaotropic and kosmotropic ions. In such a case both dipole moment and quadrupole moments of the RC must be considered.

1. Introduction

The presence in solution of an inert electrolyte is known to screen the electrostatic interactions between charged molecules. Such a screening is effective for distances above the screening length that is defined as the reciprocal of the Debye-Hückel (D-H) parameter κ that depends on the valence Z_i and concentration C_i of all the ions in solution according to: [1,2]

$$\kappa = \sqrt{\frac{2e^2\sum_i Z_i^2 C_i}{Dk_bT}} \quad (1)$$

where T is the absolute temperature, k_b the Boltzmann's constant, D the solvent dielectric constant, and *e* the elementary charge. According to Eq. (1), κ is proportional to the square root of the ionic strength.

Accordingly, in the case of bimolecular reactions, the presence of added salt slows-down reactions involving oppositely charged reactants and speeds-up reactions involving molecules of the same charge (the "kinetic salt effect"). Such a behaviour can be described within the formalism of the transition state assuming that the presence of electrolytes changes the activity coefficients of the reactants and of the activated complex [3].

For ions obeying the Debye-Hückel (D-H) theory, the activity coefficient of the i-th ion (γ_i) depends on κ according to:

$$\ln\gamma_i = -\frac{Z_i^2e^2}{2Dk_bT}\frac{\kappa}{1+\kappa R_i} \quad (2)$$

Where R_i is the radius of the i-th ion. Eq. (2) was the foundation of most the models rationalizing the dependence of the rate of electron transfer on ionic strength. The simplest model dates back to 1922 and

* Correspondence to: M. Giustini, Chemistry Department, University of Rome "La Sapienza", Italy.
** Correspondence to: G. Palazzo, Chemistry Department, University of Bari, via Orabona 4, 70125 Bari, Italy.
E-mail addresses: mauro.giustini@uniroma1.it (M. Giustini), gerardo.palazzo@uniba.it (G. Palazzo).

http://dx.doi.org/10.1016/j.bbabio.2016.06.003
0005-2728/

is the Brønsted-Debye-Hückel equation often reported in the chemical kinetics textbooks to explain the "kinetic salt effect". Such a model has been subsequently refined to handle complex reactants such as proteins [4–6].

A slightly different approach was proposed by Wherland & Gray that incorporated in the Marcus theory of electron transfer (ET) the electrostatic energy of the charged reactants within the activated complex [7].

It must be emphasized that in case of zwitterions or proteins in a charge separated state, the overall charge is null ($Z_i = 0$) and the above reviewed models foretell that the reaction rate must be independent on the ionic strength.

Several improvements have been proposed to take into account, beside the interactions among net excess charges (monopoles) also interactions involving dipole moments of the proteins (see for example the references [4–6]).

The leading contribution in these models is the monopole term and the contribution of dipole moments influences mainly the reactant mutual orientation within the activated complex.

Such models have been extensively used to study electron transfer reactions between proteins and between proteins and small ligands and the study of bimolecular reaction rates as a function the ionic strength has been proposed as a tool to disentangle electrostatic and non-electrostatic contribution to the activation free energy [3]. A non-exhaustive list of examples are the electron transfer reactions between the following pairs: cytochrome c and inorganic complexes [7], self-exchange between oxidized and reduced cytochrome b_5, [8] Cytochrome c_2 and Cytochrome bc_1, [9] Cytochrome c and Cytochrome c Oxidase, [10] Photosystem 1 and Plastocyanin, [11] Plastocyanine and Cytochrome c, [12]. Also studied was the influence of ionic strength on the electron transfer from Cytochrome c2 to the photosynthetic Reaction Center [13,14].

The subject of the latter study, the Reaction Center (RC) is the membrane-bound protein responsible, in the photosynthetic bacteria, for the initial light-induced electron transfer reaction in photosynthesis [15–17].

In the RC, photon absorption promotes electron transfer from a bacteriochlorophyll dimer pair (P) acting as the primary electron donor to the primary acceptor, Q_A, a ubiquinone molecule bound at a site close to the opposite side of the complex. This primary charge separation is stabilized by electron transfer from Q_A^- to a second ubiquinone molecule, bound at the Q_B site of the RC, which is located symmetrically to the Q_A site on the same cytoplasmic side of the membrane. In vivo, the photoxidized donor, P^+, is rapidly re-reduced by a soluble cytochrome c2, so that a second charge separation can take place across the RC, leading to the double reduction and protonation of Q_B, which leaves the RC in its quinol state, QH_2 [15,16].

The RC is yet the testing ground for the understanding of biological electron transfer because, beside the above mentioned electron transfer to cytochrome c2, it is the chief-actor of several intra-protein electron transfer reactions [16–18]. It should be noted that both the photo-induced forward charge separation ($h\nu + PQ \rightarrow P^+Q^-$) and the dark charge recombination ($P^+Q^- \rightarrow PQ$) that take place under some conditions cannot be described by the models developed for bimolecular electron transfer. Indeed, these are monomolecular ET reactions taking place among fixed redox centers within the same protein. The single reactant/product is overall neutral although it can contain separated charges.

Accordingly, the possible influence of ionic strength on these intra-protein charge recombination has been one of the few aspects of the RC functioning that was not investigated in detail. Only few non-systematic investigations, by Maroti et al., somehow addressed this point almost two decades ago [19–21].

In general, the impact of the surrounding on monomolecular intra-protein ET is an hot topic and a coupling mediated through the mechanical or dielectric response of the milieu [22–26], the chemical nature of the detergents [27] or through the solvent activity [28] was proven in the case of RC.

The purpose of the present investigation is to explore the *electrostatic* coupling between the ionic atmosphere surrounding the protein RC and the charge recombination processes taking place inside it. This has been tackled by studying the rate of charge recombination as a function of the ionic strength using as added salt the chlorides of the alkali metals (first group in the Periodic Table). The use of different salts is required in order to discriminate between the orthodox electrostatic effects implicit in the standard D-H treatment where the only difference among ions with the same valence is their size and the so called ion-specific effects [29,30]. A specific influence of the non-electrostatic nature of ions is presently assessed for several aspects of protein functionality and the effectiveness of different ions can be ordered according to the series first described by Franz Hofmeister, in the last decades of XIX century, that classified salts on the basis of their ability to solubilise or precipitate a water soluble protein [31]. The impact of ion nature on ion-specific effects depends on their degree of hydration. A traditional classification divides the ions into two families: ions with a high degree of hydration are called *kosmotropic* ions while those with a low degree of hydration are said *chaotropic* ions [29].

2. Experimental

RCs from *Rhodobacter sphaeroides* were isolated and purified according to Gray et al. [32]. In all preparations, the ratio of the absorption at 280 and 800 nm was between 1.2 and 1.3. This isolation procedure provides RCs with a Q_B content of about 60%.

RC was suspended in 10 mM Tris-HCl buffer at pH = 8.00, Lauryl-Dimethyl-Amino-Oxide (LDAO) 0.025% (w/v), hereafter TL buffer.

For each salt studied, two RC buffered mother solutions have been prepared; namely, one at the maximum salt concentration (see further) and one with buffer only, both at the same RC concentration ($1.0 \le [RC] \le 1.7$ μM, depending on RC batch of purification). These two solutions represent the extremes of the concentration interval explored, the intermediate solutions being prepared by properly mixing the two. This strategy not only allowed the minimization of RC concentration differences among samples but also ensured the reproducibility of the sample preparations. The RC concentration in each sample has been checked by Vis spectroscopy being known its molar extinction coefficient at 802 nm ($\varepsilon_{802\ nm} = 0.288\ \mu M^{-1}\ cm^{-1}$), a band not influenced by the RC redox state. For the fluorescence measurements, samples were diluted to have a [RC] ≅ 0.1 μM in order to minimize self screening effects.

Chloride salts of alkali metals have been used in order to cover a wide range in kosmotropic and chaotropic ions within the Hofmeister series. The reduced KCl solubility in the presence of LDAO (4.59 M in pure water; 3.20 M in TL) constrains its maximum concentration at 3.20 M for all the other salts the maximum concentration was 4.00 M.

After the measurements, the samples at [salt] = 1.00 M, were dialyzed (3 kDa cut-off dialysis membrane) against TL buffer for about 24 h with two changes of buffer (in any case the volume ratio was 1:100) to check the reversibility of any ions' effect on the protein. The efficiency of the dialysis procedure was checked by measuring the conductivity of the dialysis buffer. The buffer after the second dialysis showed in any case conductivity values typical of the TL buffer alone.

The activity of water (a_W) of the different salts' solutions were measured at 25 °C by means of a water activity meter (PA_wkit, Decagon Devices Inc.) previously calibrated with suitable standards (tolerance ± 0.02 a_W).

UV–Vis-Near IR spectra have been acquired with a Varian Cary-1 spectrophotometer.

Light induced redox changes of the primary donor of RC were monitored by a home-built kinetic single beam spectrophotometer

realized with an orthogonal geometry between the measuring (870 nm) and exciting (532 nm) laser beams. Details on this instrumentation have been given elsewhere [33,34]. Care has been paid to keep the measuring beam intensity as low as possible in order to minimize the excitation of the sample by the measuring light itself [35]. Temperature was controlled (25.0 ± 0.2 °C) by a water circulating bath.

Details on the steady-state and time resolved fluorescence experiments are reported in the Supporting Information.

3. Results

The functionality of the RC in presence of excess salt has been tested by studying the light-induced charge separation and the subsequent recombination reactions in single-turnover experiments. Following a flash of light, an electron is delivered in about 200 ps from the primary donor P to the primary quinone acceptor Q_A, forming the charge separated state $P^+Q_A^-$. When a second quinone molecule is bound at the secondary acceptor site Q_B, in about 100 μs it receives the electron from Q_A^-, yielding the $P^+Q_B^-$ state. In the absence of electron donors to P^+, the electron on Q_B (or Q_A) recombines with the hole on the primary donor, as shown by the following scheme [15–17].

Under physiological conditions, the rate of the $P^+Q_A^-$ recombination ($k_f \approx 10\ s^{-1}$) is slower than the rate of protein conformational changes and the non-ergodicity effects that dominate the fast charge separation [36] are absent and the reactions described in the Scheme 1 can be treated classically. In addition, the ET between the two quinones is much faster than the $P^+Q_A^-$ recombination and the concentration of the species $P^+Q_A^-Q_B$ and $P^+Q_AQ_B^-$ is governed by the equilibrium constant L_{AB} [37]. Charge recombination of the $P^+Q_AQ_B^-$ state occurs essentially by thermal repopulation of $P^+Q_A^-Q_B$ state with an observable overall rate constant $k_s \approx 1\ s^{-1}$, which is determined by the values of k_f and L_{AB} [37,38].

Upon purification, a certain amount of quinone at the Q_B site is lost. In RC depleted of quinone at Q_B site, P^+ decays faster according to Scheme 2:

As a consequence, the decay of P^+ following a short photoexcitation includes in general two kinetic components, a fast and a slow one, ascribed to RC subpopulations which undergo $P^+Q_A^-$ and $P^+Q_AQ_B^-$ recombination respectively. According to the schemes above, kinetic analysis of charge recombination yields information on $P^+Q_A^-$ recombination as well as on electron transfer from Q_A^- to Q_B.

Since the P and P^+ have different extinction coefficients at 870 nm, the transient flash-induced formation of P^+ and its subsequent decay by charge recombination can be monitored at this wavelengths. Representative time courses of absorption changes after the laser pulse are shown in Fig. 1 for RCs in presence of increasing amounts of NaCl. A deceleration of the slow exponential phase of the charge recombination process upon increasing the salt concentration is clearly visible (in the semi-log representation of Fig. 1, the slope of the long-time linear region decreases). This behaviour is qualitatively shared by RCs dissolved in KCl, CsCl, RbCl. A notable exception is represented by LiCl where, as shown in Fig. 2, the overall P^+ decay is faster at [LiCl] = 4 M than at [LiCl] = 1 M. In addition, the long-time decay deviates markedly from the single exponential.

Often, the slow phase kinetics are not accounted for by a single value of the relevant kinetic constant rather by a spread of values that reflects heterogeneity in the nature of the Q_B site.

Several models have been proposed to account for the distributed kinetic phases of charge recombination [22,23,39,40].

$$PQ_AQ_B \underset{k_f}{\overset{h\nu}{\leftrightarrows}} P^+Q_A^-Q_B \overset{L_{AB}}{\longleftrightarrow} P^+Q_AQ_B^-$$

Scheme 1. Photo-induced charge separation and charge recombination from Q_B.

$$PQ_AQ_B \underset{k_f}{\overset{h\nu}{\leftrightarrows}} P^+Q_A^-$$

Scheme 2. Photo-induced charge separation and charge recombination from Q_A.

Here we have found that the whole charge recombination process is adequately accounted for, in terms of both χ^2 and residuals, by the sum of an exponential decay (fast phase) and of a power law (slow phase): [23,40]

$$\frac{\Delta Abs_{870\ nm}(t)}{\Delta Abs_{870\ nm}(0)} = X_f e^{-k_f t} + \frac{1-X_f}{(1+\varphi_s t)^{n_s}} \quad (3)$$

where the subscripts *f* and *s* identify, respectively, the fast and the slow phase of the whole charge recombination process and X_f is the fraction of RC with the Q_B site empty. With respect to the slow process, φ_s and n_s are parameters describing the spread of the slow kinetics. In particular, φ_s and n_s are related to the average ($\bar{k}_s$) and to the variance σ^2 of the rate constants via the relationships $\bar{k}_s = \varphi_s \cdot n_s$, and $\sigma^2 = \varphi_s^2 n_s$ [26].

Accordingly, the experimental decays have been fitted to Eq. (3) and the best fit parameters are listed in Table 1 (RCs in TL) and Table 2(RCs in presence of added salts).

In order to better understand the RC kinetic behaviour upon varying the salts' nature and concentration, the data will be analyzed and discussed separately for the $P^+Q_A^-$ charge recombination (fast component) and for the $P^+Q_A^-Q_B \rightleftarrows P^+Q_AQ_B^-$ ET (linked to the slow component).

3.1. $P^+Q_A^-$ charge recombination process

In Fig. 3 is shown the logarithm of the rate constant k_f, associated with the fast component of the charge recombination ($P^+Q_A^- \rightarrow PQ_A$) as a function of the D-H parameter κ (defined by the Eq. (1)) that is proportional to the square root of the salt concentration.

Upon increasing κ, k_f shows an increase in its value; this behaviour being shared by all the cations studied. For Na^+, K^+, Rb^+ and Cs^+, this leads to mutually close values of the rate constant. In the case of Li^+, the qualitative behaviour is the same though the increase in k_f is more pronounced.

The ET process from the charge separated state $P^+Q_A^-$ to PQ_A takes place through direct tunnelling, and changes in its rate can be ascribed to modification in the energetics or in the protein and/or cofactor distance and reciprocal orientation. If the latter would be the case, fluorescence measurements, should probe such variations as modifications in the spectra and/or in the fluorescence lifetimes. In particular, the emission of the bacteriopheophytin centred around 762 nm strongly

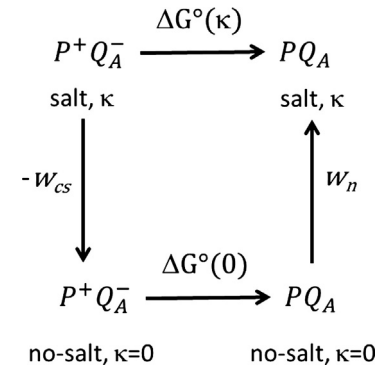

Scheme 3. Thermodynamic cycle to account for the $P^+Q_A^-$ charge recombination in salt solution.

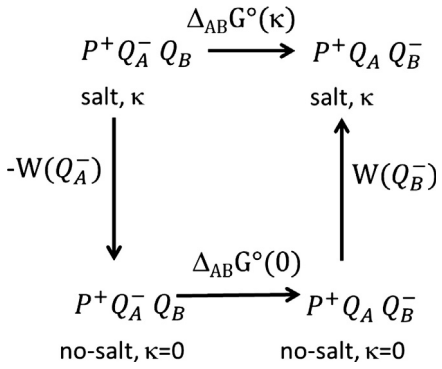

Scheme 4. Thermodynamic cycle to account for the $P^+Q_AQ_B \rightarrow P^+Q_AQ_B$ET in salt solution.

overlaps the absorption band of the monomeric bacteriochlorophyll and any change in the relative distance/orientation between these pigments should change the fluorescence intensity and lifetime. As it is shown in the Supporting Information, such alterations in the fluorescence parameters were not observed even in the case of high (4.00 M) salts concentrations.

Having ruled out changes in the geometry of the donor-acceptor pair, the rationale of the salt-induced acceleration of the charge recombination effect must be due to an influence of the ionic atmosphere on the energetics of the process.

The charge separated species involved in the $P^+Q_A^- \rightarrow PQ_A$ process hold no net charge (monopole) and as such cannot be treated using the orthodox formalism developed for reaction between ions.

Species like $P^+Q_A^-$ could be described instead as transient zwitterions. In 1934 Kirkwood solved, in closed form, the electrical contribution to the chemical potential of a zwitterion. Strictly the Kirkwood's approach is quite general and takes into account the presence of electrical monopoles, dipoles and higher order multipoles (details are given in the SI) giving the chemical potential of a particle containing an arbitrary distribution of charges within a spherical domain of low dielectric constant immersed in a solvent at high dielectric constant.

He calculated the free energy change associated to the particle transfer from a solution at null ionic strength ($\kappa = 0$) to a solution of salt characterized by a D-H parameter κ. Applying such a model to the RC thought as a large zwitterion that has not net charge but only an

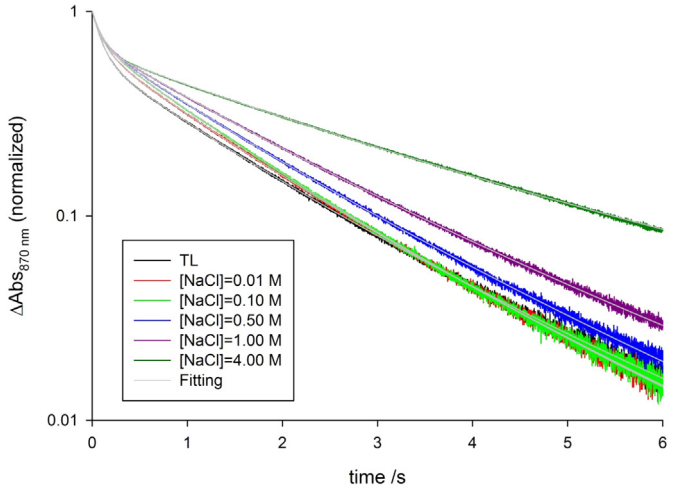

Fig. 1. Kinetics of charge recombination of RC after a laser pulse fired at t = 0 at different NaCl concentrations. Conditions: T = 25.0 ± 0.2 °C; time resolution 0.1 ms. Also shown are the fits of the data to Eq. (3).

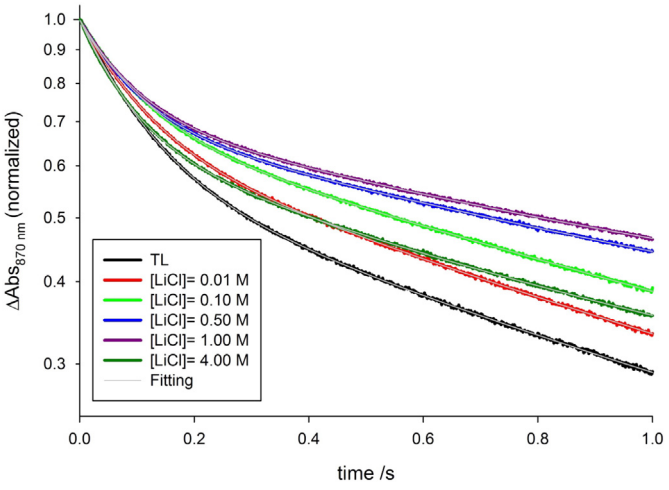

Fig. 2. Kinetics of charge recombination of RC after a laser pulse fired at t = 0 at different LiCl concentrations. Conditions: T = 25.0 ± 0.2 °C; time resolution 0.1 ms. Also shown are the fits of the data to Eq. (3).

electrical dipole moment, the free energy associated to the transfer from pure water ($\kappa = 0$) to salt solution (κ) is

$$w(a, P, \kappa) = -\frac{\kappa^2}{2D}\left[\frac{3P^2}{4a\left(1 + \kappa a + \frac{(\kappa a)^2}{2}\right)}\right] \quad (4)$$

Where *a* is the radius of the low dielectric constant domain inaccessible to the ions (roughly the protein radius) and *P* is the overall dipole moment.

The Kirkwood's transfer free energy can be used to rationalize the dependence on ionic strength of k_f considering the thermodynamic cycle shown in Scheme 3.

The $P^+Q_A^- \rightarrow PQ_A$ process taking place in the salt solution at D-H parameter κ is described by three intermediate step. In the first the *charge separated* $P^+Q_A^-$ protein is removed from the salt solution and placed in pure water ($\kappa = 0$) with a free energy cost equal to $-w_{cs}$. The ET is performed in pure water with a free energy change $\Delta G°(0)$ and finally the *neutral* PQ_A protein is transferred back from the pure water to the salt solution with an energy change w_n. Therefore the driving force for the charge recombination in salt solution is $\Delta G°(\kappa) = \Delta G°(0) - w_{cs} + w_n = \Delta G°(0) - \Delta w$.

This is related to the observed rate constant k_f according to the Marcus ET theory that foretells that $k_f = \frac{2\pi}{\hbar}|V|^2 \exp[\frac{-(\Delta G° + \lambda)^2}{4\lambda k_b T}]$ where λ is the reorganization energy, and $|V|^2$ is the electronic exchange matrix element that, depending only on the donor-acceptor distance, is independent on the ionic strength [41,42]. Accordingly, the rate constant in salt solution is:

$$k_f(\kappa) = \frac{2\pi}{\hbar}|V|^2 \exp\left[\frac{-(\Delta G°(0) - \Delta w + \lambda)^2}{4\lambda k_b T}\right] \quad (5)$$

Experimentally, the rate of the ET from Q_A^- to P^+ reaches the highest value at high ionic strength (Fig. 3) reaching a value $k_f^{max} \approx 10.8\ s^{-1}$ for all the salts but LiCl for which it is slightly larger ($k_f^{max} = 12.0\ s^{-1}$). According to Eq. (5), the maximum rate ($k_f{}^{max} = \frac{2\pi}{\hbar}|V|^2$) is observed when the reaction driving force matches the reorganization energy of the electron transfer ($\Delta G°(0) - \Delta w^{max} = -\lambda$). On the other

Table 1
Characteristic parameters of RCs charge recombination in TL buffer in absence of added salt.

Ionic strength/M	0.005
κ/nm^{-1}	0.23
k_f/s^{-1}	8.79 ± 0.01
$\overline{k}_s/s^{-1}$	0.76 ± 0.01
σ^2/s^{-2}	0.064 ± 0.001
X_f	0.42 ± 0.02
L_{AB}	10.6 ± 0.1
$\Delta_{AB}G°/kT$	−2.36 ± 0.1

hand, at low ionic strength $\Delta w \approx 0$ and the rate constant is $k_f{}^\circ = \frac{2\pi}{h}|V|^2 \exp[\frac{-(\Delta G^\circ(0)+\lambda)^2}{4\lambda k_b T}]$. According to the relations holding at low and high ionic strength one can describes the term $\Delta G^\circ(0) + \lambda = \Delta w^{max}$ as a function of the rate constants at zero and at high ionic strength:

$$\Delta G^\circ(0) + \lambda = \sqrt{4\lambda k_b T \ln\left(\frac{k_f^{max}}{k_f^0}\right)} \tag{6}$$

Combining Eqs. (5) and (6) yields

$$\ln k_f(\kappa) = \ln k^\circ{}_f - \ln\left(\frac{k_f^{max}}{k_f^0}\right)\frac{\Delta w}{\sqrt{\lambda k_b T}} - \frac{\Delta w^2}{4\lambda k_b T} \tag{7}$$

Assuming that both w_{cs} and w_n are described by Eq. (4) and considering that the size a of the RC remains constant the term Δw can be rewritten as

$$\Delta w = -\frac{\kappa^2}{2D}\left[\frac{3\Delta P^2}{4a\left(1+\kappa a+\frac{(\kappa a)^2}{2}\right)}\right] \tag{8}$$

Where ΔP^2 is the difference between the square of the dipole moments of $P^+Q_A^-$ and PQ_A states.

The data of Fig. 3 have been therefore fitted to Eqs. (7) and (8), leaving as adjustable parameters only the protein radius a and ΔP^2. The following parameters where used in the best-fit: $k_f{}^\circ = 8.8\ s^{-1}$ and $\lambda = 0.5$ eV [42] for all the salts; $k_f^{max} = 12.0\ s^{-1}$ was used for LiCl and $k_f^{max} = 10.8\ s^{-1}$ for all the remaining salts.

The best fit parameters are listed in Table 3 for the different salts.

Inspection of Table 3 reveals that either the size of the low dielectric domain a or the dipole moment are independent on the nature of the salt.

The average size of the low dielectric domain a is 0.86 nm with a standard deviation of 0.3 nm. This is smaller than the RC size at least by a factor 5. Such an incongruity cannot be related to the numerical value of λ used because it has negligible effect on the best-fit parameter a while it impacts strongly on the ΔP^2-parameter. We retain that the

Table 2
Characteristic parameters of RCs charge recombination in TL buffer in presence of added salt.

[salt]/M	0.01	0.1	0.5	1.0	3.2	4.0
Ionic strength/M	0.015	0.105	0.005	1.005	3.205	4.005
κ/nm^{-1}	0.40	1.06	2.34	3.30	5.89	6.58
LiCl						
k_f/s^{-1}	9.30 ± 0.02	9.50 ± 0.02	10.40 ± 0.02	10.81 ± 0.02	–	11.9 ± 0.1
$\overline{k}_s/s^{-1}$	0.74 ± 0.01	0.62 ± 0.01	0.52 ± 0.05	0.54 ± 0.05	–	0.82 ± 0.01
σ^2/s^{-2}	0.044 ± 0.001	0.034 ± 0.001	0.026 ± 0.001	0.026 ± 0.001	–	0.52 ± 0.01
X_f	0.35 ± 0.01	0.30 ± 0.01	0.30 ± 0.01	0.28 ± 0.01	–	0.33 ± 0.01
L_{AB}	11.5 ± 0.2	14.3 ± 0.1	18.9 ± 0.2	18.9 ± 0.2	–	13.5 ± 0.2
$\Delta_{AB}G°/kT$	−2.44 ± 0.01	−2.66 ± 0.01	−2.94 ± 0.01	−2.94 ± 0.01	–	−2.60 ± 0.01
NaCl						
k_f/s^{-1}	8.87 ± 0.02	9.51 ± 0.01	9.97 ± 0.01	10.37 ± 0.01		10.72 ± 0.01
$\overline{k}_s/s^{-1}$	0.76 ± 0.01	0.79 ± 0.01	0.70 ± 0.01	0.61 ± 0.01		0.39 ± 0.01
σ/s^{-1}	0.25 ± 0.01	0.26 ± 0.01	0.22 ± 0.01	0.20 ± 0.01		0.16 ± 0.01
X_f	0.335 ± 0.003	0.290 ± 0.003	0.300 ± 0.003	0.300 ± 0.003		0.355 ± 0.003
L_{AB}	10.7 ± 0.1	11.0 ± 0.1	13.2 ± 0.1	16.0 ± 0.2		26.5 ± 0.3
$\Delta_{AB}G°/kT$	−2.36 ± 0.01	−2.40 ± 0.01	−2.58 ± 0.01	−2.77 ± 0.01		−3.28 ± 0.01
KCl						
k_f/s^{-1}	8.93 ± 0.01	9.50 ± 0.01	10.00 ± 0.01	10.11 ± 0.01	10.66 ± 0.01	–
$\overline{k}_s/s^{-1}$	0.801 ± 0.01	0.85 ± 0.01	0.81 ± 0.01	0.76 ± 0.01	0.55 ± 0.01	
σ/s^{-1}	0.26 ± 0.01	0.28 ± 0.01	0.26 ± 0.01	0.23 ± 0.01	0.20 ± 0.01	
X_f	0.344 ± 0.003	0.285 ± 0.003	0.88 ± 0.003	0.298 ± 0.003	±0.003	
L_{AB}	10.1 ± 0.1	10.2 ± 0.1	11.3 ± 0.1	12.3 ± 0.1	18.4 ± 0.2	
$\Delta_{AB}G°/kT$	−2.31 ± 0.01	−2.32 ± 0.01	−2.43 ± 0.01	−2.51 ± 0.01	−2.91 ± 0.01	
RbCl						
k_f/s^{-1}	8.91 ± 0.01	9.36 ± 0.01	9.91 ± 0.02	10.22 ± 0.02	–	10.92 ± 0.02
$\overline{k}_s/s^{-1}$	0.78 ± 0.01	0.82 ± 0.01	0.8 ± 0.01	0.76 ± 0.01		0.54 ± 0.01
σ/s^{-1}	0.24 ± 0.01	0.23 ± 0.01	0.23 ± 0.01	0.23 ± 0.01		0.16 ± 0.01
X_f	0.37 ± 0.01	0.31 ± 0.01	0.31 ± 0.01	0.32 ± 0.01	–	0.35 ± 0.01
L_{AB}	10.4 ± 0.1	10.4 ± 0.2	11.4 ± 0.2	12.4 ± 0.2		19.2 ± 0.3
$\Delta_{AB}G°/kT$	−2.34 ± 0.01	−2.34 ± 0.01	−2.4	−2.52 ± 0.01		−2.96 ± 0.02
CsCl						
k_f/s^{-1}	8.98 ± 0.01	9.53 ± 0.01	10.11 ± 0.01	10.23 ± 0.01		10.60 ± 0.01
$\overline{k}_s/s^{-1}$	0.82 ± 0.01	0.88 ± 0.01	0.85 ± 0.01	0.78 ± 0.01		0.53 ± 0.01
σ/s^{-1}	0.27 ± 0.02	0.28 ± 0.02	0.29 ± 0.02	0.26 ± 0.02		0.20 ± 0.02
X_f	0.36 ± 0.01	0.32 ± 0.01	0.32 ± 0.01	0.32 ± 0.01		0.35 ± 0.01
L_{AB}	9.9 ± 0.1	9.8 ± 0.1	10.9 ± 0.1	12.1 ± 0.1		18.9 ± 0.2
$\Delta_{AB}G°/kT$	−2.29 ± 0.01	−2.30 ± 0.01	−2.39 ± 0.01	−2.49 ± 0.01		−2.94 ± 0.01

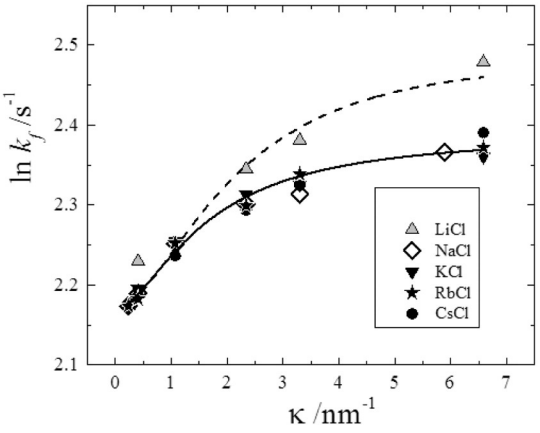

Fig. 3. Dependence of the rate constant of P^+QA^- charge recombination k_f on the Debye-Hückel parameter κ defined in Eq. (1). Lines are the best fit of data for LiCl (dashed) and NaCl (solid) to Eqs. (7) and (8); the fits for the other salts are indistinguishable from the NaCl case. The best-fit values are listed in Table 2. In the case of NaCl the fixed parameters are $k_f^\circ = 8.8\ s^{-1}$, $k_f^{max} = 10.8\ s^{-1}$, λ = 0.5 eV. In the case of LiCl the fixed parameters are $k_f^\circ = 8.8\ s^{-1}$, $k_f^{max} = 12.0\ s^{-1}$, λ = 0.5 eV.

low values of the *a* parameter are likely related to the approximation on the value of the protein internal dielectric constant implicit in the Kirkwood's treatment. The numerical prefactors of *a* in Eq. (4) have been evaluated under the assumption of a dielectric constant that is homogenous within the protein and assuming that the ratio between the dielectric constant of the protein and of the solvent is negligible. These assumptions are a poor description of the local dielectric properties of the RC in which the relative dielectric constant is believed to be a function of the position and can reach values around 25–40 [18].

According to Table 3, the ΔP^2 is always positive meaning that the dipole on $P^+Q_A^-$ is larger than that on PQ_A as it is expected. In the reasonable case the dipole on $P^+Q_A^-$ is much larger than that on PQ_A, we can neglect this latter and $(\Delta P^2)^{1/2}$ equals the overall dipole moment of the RC in the charge separated state. The center-to-center distance between P^+ and Q_A^- is 28 Å [43] and this means that the photoinduced $P^+Q_A^-$ charge separation contributes to the dipole moment with ≈+134 debyes. The $(\Delta P^2)^{1/2}$ values, ranging from +65 debye to 150 debye (see Table 3), are thus in perfect agreement with such an estimate (the mean value is 103 debye with a standard deviation of 36 debye).

3.2. $P^+Q_AQ_B^-$ charge recombination process

In the case of the rate constant of the slow kinetic phase (k_s), the effect of the salt concentration is strongly dependent on the nature of the cation. For Na^+, K^+, Rb^+, Cs^+ up to 0.10 M, k_s slightly grows upon salt loading (Tables 1 and 2) but such an increase remains below 15%. However, for further increase in the salt content from 1.0 M to 4.0 M, the k_s value significantly drops.

Inspection of Tables 1 and 2, indicates that the presence K^+, Rb^+ and Cs^+, roughly induces the same decrease in k_s at a given salt concentration. In the case of sodium cation the decrease in k_s is more pronounced. For Li^+, the situation is completely different and, even at the lowest concentration, strong deviations from the behaviour of the other alkaline cations were observed, with a steep decrease of k_s that, after reaching its minimum value at $[Li^+] = 0.50$ M, steeply recovers its typical value in TL buffer for $[Li^+] = 4.0$ M. It is interesting to point out that the spread of the slow kinetic phase for Li^+ is always higher than that observed for the other cations (see Table 2) and the standard deviation σ of the slow phase reaches the same order of magnitude of k_s value itself at $[Li^+] = 4.0$ M (see Table 2). Such a huge value of σ suggests the presence of multiple adsorption sites for Li^+ resulting in a high heterogeneity in the electric charge distribution as has been already observed in RC incorporated in the cationic polymer poly(dimethyldiallylammonium) chloride (PDDA) matrices [44].

Table 3
Best Fit *a* and ΔP^2 values obtained from the dependence of the $P^+Q_A^-$ charge recombination rate on the ionic strength.

Salt	*a*/nm	ΔP^2/debye^2	$\sqrt{\Delta P^2}$/debye
LiCl	0.6 ± 0.2	(5 ± 4) × 10^3	70 ± 30
NaCl	0.9 ± 0.2	(12 ± 4) × 10^3	110 ± 20
KCl	1.0 ± 0.2	(15 ± 5) × 10^3	120 ± 20
RbCl	0.6 ± 0.1	(4 ± 2) × 10^3	65 ± 15
CsCl	1.2 ± 0.1	(24 ± 5) × 10^3	150 ± 15

To check the reversibility of the ion-induced effects on RC, all the samples at [salt] = 1.00 M have been extensively dialyzed against the buffer. For all the salts studied but for LiCl, after the dialysis the kinetic parameters revert back to the values assumed in TL buffer. At variance, in the case of LiCl even prolonged dialysis (>48 h and with several buffer changes) fails to recover the initial value of rate constant. Therefore, instead of a mere electrostatic adsorption on the RC surface, in the case of lithium ions it seems that there is the presence of a strong binding of the Li^+ to the protein.

A recent study using Nanoparticle Enhanced Laser-Induced Breakdown Spectroscopy (NE-LIBS), [45] revealed the presence of a large amount of cations in extensively dialyzed RC samples only in the case of Li^+.

According to Scheme 1, the rate of the $P^+Q_AQ_B^-$ charge recombination depends on the $P^+Q_A^-Q_B \leftrightarrow P^+Q_AQ_B^-$ thermodynamic equilibrium. Accordingly, the equilibrium constant L_{AB} can be evaluated using the k_f and k_s values of Tables 1 and 2 as [37,38]

$$L_{AB} = \frac{k_f}{k_s} - 1 \tag{9}$$

The corresponding free energy for the $P^+Q_A^-Q_B \rightleftarrows P^+Q_AQ_B^-$ electron transfer is easily calculated for each salt concentration according to

$$\frac{\Delta_{AB}G^\circ(\kappa)}{k_bT} = -\ln(L_{AB}) \tag{10}$$

The numerical values of L_{AB} and $\Delta_{AB}G^\circ$ are also listed in Tables 1 and 2.

The exposure to increasing concentrations of salts affects both k_f and k_s in a complex fashion and will therefore reflect also on $\Delta_{AB}G^\circ$. The dependence of $\Delta_{AB}G^\circ$ on the D-H parameter is graphically shown in Fig. 4. It can be seen that, for the "chaotropic" ions Rb^+, Cs^+, and K^+ the increase in ionic strength first makes $\Delta_{AB}G^\circ$ slightly less negative and then for concentration larger than 0.1 M the free energy decreases. Therefore, the overall trend has a maximum at $\kappa = 1\ nm^{-1}$.

Turning to sodium cation, the maximum at low concentration vanishes and only a strong decrease in free energy is observed, reaching a stabilization of the $P^+Q_AQ_B^-$ species of 0.9 k_bT compared with the salt free solution.

In the case of Li^+, the stabilization of the $P^+Q_AQ_B^-$ is very efficient already at low concentration but starts to decrease ($\Delta_{AB}G^\circ$ becomes less negative) for concentrations above 1 M ($\kappa = 3.3\ nm^{-1}$).

The $P^+Q_A^-Q_B \leftrightarrow P^+Q_AQ_B^-$ equilibrium can be treated with the help of the thermodynamic cycle shown in Scheme 4.

The ET between Q_A^- and Q_B^- in a salt solution at D-H parameter κ, is described by three intermediate steps: i) $P^+Q_A^-Q_B$ is removed from the salt solution and placed in pure water (κ = 0) with a free energy cost equal to $-W(Q_A^-)$; ii) The ET is performed in pure water with a free energy change $\Delta_{AB}G^\circ(o)$; iii) $P^+Q_AQ_B^-$ is transferred back from the pure water to the salt solution with an energy change $W(Q_B^-)$.

Therefore the free energy change for the interquinone ET in salt solution is $\Delta_{AB}G^\circ(\kappa) = \Delta_{AB}G^\circ(o) - W(Q_A^-) + W(Q_B^-) = \Delta_{AB}G^\circ(o) + \Delta_{AB}W$.

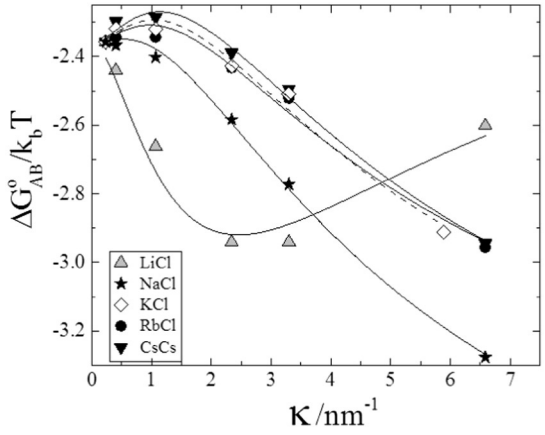

Fig. 4. Dependence of the free energy change for the reaction $P^+Q_A^-Q_B \rightleftarrows P^+Q_AQ_B^-$ ($\Delta_{AB}G^\circ$) on the Debye-Hückel parameter κ defined in Eq. (1). Lines are the best fit to Eq. (12) with the fixed parameters $\Delta_{AB}G^\circ(0) = -2.36\ k_bT$, $a = 0.86$ nm.

The effect of ionic strength on this thermodynamic equilibrium is less easy to grasp than that on the kinetic rate of charge recombination previously described (Section 3.1). Here there is not a dipole that vanishes but instead a change in the orientation of the charges and, due to the mirror symmetry of the cofactors in the RC, the distance between P^+ and the negative charge doesn't change when the electron passes from Q_A^- to Q_B^-. In spite of this consideration, $\Delta_{AB}G^\circ$ is strongly dependent on κ. A further striking evidence is that $\Delta_{AB}G^\circ$ clearly depends on κ differently in the case of chaotropic and kosmotropic ions. A possibility to reconcile such an experimental evidence with the Kirkwood's treatment that doesn't contain any parameter that explicitly depends on the nature of the ions, is that different ions adsorb differently on the RC and thus they contribute differently to the multipole moments of $P^+Q_A^-Q_B$ and $P^+Q_AQ_B^-$. Our hypothesis is that the non-electrostatic ion-specific interactions rule the ion binding and thus tune the charge distribution within the protein while the electrostatics determines how the ionic atmosphere screens these charges.

Any attempt to describe this behaviour in terms of dipole contribution only (i.e. by fitting the data of Fig. 4 to Eq. (8)) cannot reproduce the minimum observed in the case of Li^+ and the shallow maximum found for Rb^+, Cs^+, K^+ because in Eq. (8) the energy can only change monotonically with κ. To describe the phenomenology shown in Fig. 4 we have to describe the electrostatics of the RC including also the quadrupole terms. The Kirkwood formula including the quadrupole contributions is recalled in the SI, and here we use directly the final result. In this case, the free energy associated to the transfer of a generic protein from $\kappa = 0$ to κ is

$$W = w(a, P, \kappa) + Q^2 f(a, \kappa) \tag{11}$$

The dipole contribution to the energy $w(a, P, \kappa)$ is given by Eq. (4) and the contribution of the quadrupolar terms is given by the product between the function $f(a, \kappa)$ (that depends on the size of the low dielectric domain a and on κ) and the square of the quadrupole moment Q.

In the process $P^+Q_A^-Q_B \rightarrow P^+Q_AQ_B^-$ the a-parameter is expected to be constant. Therefore it is possible to write

$$\Delta_{AB}G^\circ(\kappa) = \Delta_{AB}G^\circ(0) - \frac{\kappa^2}{2D}\left[\frac{3\Delta P^2}{4a\left(1 + \kappa a + \frac{(\kappa a)^2}{2}\right)}\right] + \Delta Q^2 f(a, \kappa) \tag{12}$$

Where ΔQ^2 is the difference in the squares of the quadrupole moment for $P^+Q_A^-Q_B$ and $P^+Q_AQ_B^-$ and the analytical form of $f(a, \kappa)$ is given in the SI.

The data of Fig. 3 have been first fitted to Eq. (12) leaving three adjustable parameters, namely: a, ΔP^2, and ΔQ^2; $\Delta_{AB}G^\circ(0)$ was fixed to the value found in absence of added salt (Table 1). The description in terms of charge screening on the dipole and quadrupole moments successfully describes the large variety of dependence of $\Delta_{AB}G^\circ$ on κ including the minimum observed for Li^+ and the maximum observed for Cs^+, Rb^+, and K^+ (see fits in Fig. S9 SI). The a, ΔP^2, and ΔQ^2 best-fit parameters are listed in Table S1 in the SI. It turned out that the values of the parameter a coincide within the error with those obtained in the analysis of the $P^+Q_A^-$ charge recombination kinetics (Table 3). With respect to the changes in the dipole and quadrupole moments, Na^+, K^+, Rb^+ and Cs^+ have negative ΔP^2 and positive ΔQ^2 values although the large uncertainties associated to a fit with three adjustable parameters overcast any differences due to the nature of the ions. A notable exception is represented again by the case Li^+ where positive ΔP^2 and negative ΔQ^2 values are observed.

To reduce the uncertainty in the best-fit parameter we have therefore fixed the parameter a to the average value found in the independent analysis of the rate of $P^+Q_A^- \rightarrow PQ_A$ ($a = 0.86$ nm) and the data have been fitted to Eq. (12) with only ΔP^2 and ΔQ^2 as adjustable parameters. The resulting fits are shown in Fig. 4 and the best fit parameters listed in Table 4.

This strategy considerably reduced the uncertainties on the best-fit parameters that can be properly compared. With the exception of LiCl, the nature of the salt doesn't impact on the difference on the quadrupole moment between $P^+Q_AQ_B^-$ and $P^+Q_A^-Q_B$. The chaotropic ions K^+, Rb^+ and Cs^+ share also the same difference in the dipole moment. For these ions $\Delta P^2 = (-4 \pm 0.6) \times 10^3$ debye^2 indicating that the dipole moment on $P^+Q_AQ_B^-$ is smaller than that on $P^+Q_A^-Q_B$. Passing to the sodium ion ΔP^2 becomes 30% less negative. In presence of Li^+ the charge distribution within the RC changes drastically with a dipole moment on $P^+Q_AQ_B^-$ that is larger than that on $P^+Q_A^-Q_B$ ($\Delta P^2 = +10 \times 10^3$ debye^2) while the opposite holds for the quadrupole moment ($\Delta Q^2 < 0$).

4. Discussion

The belief that the main effect of the ionic strength on chemical reactivity is its impact on bimolecular reactions between charged pairs has overshadowed any influence on intra-protein ET. Also in the few papers (focused only on the P^+QA^- charge recombination) where an effect of the ionic atmosphere was assessed, this has been discussed in terms of binding and screening of protonatable groups (i.e. changes in the local pH and/or pKa) as dominant modes of electrostatic interaction between protein and salt [19–21].

To our best knowledge, this is the first study proving an electrostatic influence of the ionic strength on the kinetics and thermodynamics of ET processes involving opposite charges deeply buried within the same protein.

The above described experimental results unambiguously show a marked influence of the ionic atmosphere on two very different intra-protein ET processes taking place inside of the RC: i) the *kinetics* of the charge recombination from $P^+Q_A^-$; ii) the *thermodynamic equilibrium* between $P^+Q_A^-Q_B$ and $P^+Q_AQ_B^-$.

A distinctive point of the present investigation is that reactants and products of the reactions do not carry net charges and thus the leading interactions involve dipole moments that have been accounted for by

Table 4
Best Fit ΔP^2 and ΔQ^2 values obtained from the dependence of the $\Delta_{AB}G^\circ(\kappa)$ on the ionic strength keeping constant a = 0.86 nm.

Salt	ΔP^2/debye^2	$\Delta Q^2/10^{-74}$ m^{4}C^2
LiCl	$(+10 \pm 0.9) \times 10^3$	-8 ± 1
NaCl	$(-2.8 \pm 0.3) \times 10^3$	$+5.6 \pm 0.4$
KCl	$(-4.0 \pm 0.6) \times 10^3$	$+5.6 \pm 0.6$
RbCl	$(-3.6 \pm 0.6) \times 10^3$	$+5.2 \pm 0.4$
CsCl	$(-4.8 \pm 0.4) \times 10^3$	$+6.0 \pm 0.4$

the Kirkwood's equations. Such an approach furnishes a consistent description of the effect of the ionic strength on two completely different ET processes. It is worth noting that, although the two key parameters investigated are different in nature (one is the kinetic rate constant k_f the other the equilibrium free energy changes $\Delta_{AB}G^\circ$) and for this reason they depend on the ionic strength according to relations that are formally different (Eqs. (7) and (12)), they are accounted for by the same *a*-parameter. The analysis of the rate of $P^+Q_A^-$ charge recombination furnishes as best-fit parameter, averaged over all the salts, $a = 0.86 \pm 0.25$ nm while the dependence of $\Delta_{AB}G^\circ$ on the salt concentration gives $a = 0.6 \pm 0.1$ nm (value averaged over all the salts; for the individual values see Table 1S in the SI).

The rate of the $P^+Q_A^-$ charge recombination is known to be unaffected by the surrounding solution osmotic pressure and viscosity [28] and is only slightly affected by the temperature [46] (above 273 k). Also incorporation of RCs in solid glasses affects it only when the surrounding solid matrix becomes extremely rigid [22,24]. Therefore the marked effect of ionic strength (Fig. 3) on the ET from Q_A^- to P^+ is unexpected.

The Eqs. (7)–(8) ascribe the acceleration in the ET rate upon increasing the ionic strength to the negative value of the $\Delta w(\kappa)$. Due to the larger dipole moment associated to $P^+Q_A^-$ compared to PQ_A, the presence of salt stabilizes the charge separated state more than the ground state thus decreasing the free energy gap between reactants and products. In other words, upon salt loading, the $\Delta G^\circ(\kappa)$ approaches the reorganization energy (λ) from the side of the Marcus "inverted region" [41]. Overall, this is a small effect ($\approx$75 meV) but could play a role in vivo since the ionic strength of the intracellular matrix is not negligible. Remarkably, such a rationalization involves only the pure electrostatic screening of the photo-induced $P^+Q_A^-$ dipole and doesn't require any salt-induced change in the protonation state of the protein.

Since, for the $P^+Q_A^-$ charge recombination, either the size of the low dielectric domain (*a*) or the dipole moment are independent on the nature of the salt (Table 2), the influence of the ionic strength on this process must be classified as an electrostatic effect that is not ion-specific.

On the contrary, the thermodynamic equilibrium between $P^+Q_A^-Q_B$ and $P^+Q_AQ_B^-$ depends on the salt concentration in a fashion that is different for chaotropic and kosmotropic ions. It should be stressed that the high concentration of salts here used have only a moderate effect on the water activity that never goes below 0.86 (minimum value measured for a_W in the case of the LiCl 4.00 M solution). This is important because the rate of charge recombination from $P^+Q_AQ_B^-$, although associated to the release of water molecules, slows-down only when the water activity drops below 0.80 [28]. The high value of water activity in the present study rules out such an osmotic contribution to the observed stabilization of the $P^+Q_AQ_B^-$ state.

According to Table 4, the chaotropic ions K^+, Rb^+, and Cs^+ stabilize the $P^+Q_A^-Q_B \rightarrow P^+Q_AQ_B^-$ ET in the same way. The analysis of the κ-dependence of $\Delta_{AB}G^\circ(\kappa)$ indicates that, for the chlorides of these cations, the ET from Q_A^- to Q_B is associated to the same decrease of the dipole moment and to the same increase of the quadrupole moment. This indicates that, for the chaotropic cations, the effect of the added salt is essentially a non-specific electrostatic stabilization of the charge distribution within the protein. Since the $P^+Q_A^-Q_B \rightarrow P^+Q_AQ_B^-$ ET is known to be conformationally gated [47] (i.e. is governed by a protein rearrangement) the changes in the dipole and the quadrupole moments reflect the rearrangement of the protein conformation and possibly the small proton uptake which is known to stabilize the charge on Q_B as the electron passes from Q_A^- to Q_B [18].

Passing to the kosmotropic side of the alkali series, we observe that loading with Na^+ leaves unchanged the ΔQ^2 but reduces the change in the dipole moment. Eventually, exposure of the RCs to lithium ions changes drastically the inner charge distribution; the dipole moment on $P^+Q_AQ_B^-$ is now larger than that on $P^+Q_A^-Q_B$ ($\Delta P^2 > 0$) while the opposite holds for the quadrupole moment ($\Delta Q^2 < 0$). The non-reversibility of the effect of Li^+ upon dialysis indicates that lithium ions effectively bind the RC already at low concentration.

In this respect it is interesting to compare our results with the affinity of alkali cations for polypeptides and block-copolymers. In a recent investigation, Cremer and co-workers have examined the affinity of anions [48] and cations [49] for the carboxylate side chains of an elastin-like polypeptide. The authors have found the same affinity for the polypeptide in the case of chaotropic cations Cs^+, Rb^+ and K^+. The affinity between cations and the carboxylate side chains becomes stronger passing to Na^+ and reaches its maximum in the case of Li^+.

In another recent study, Zhang and co-workers have investigated the binding of alkali cations to a triblock copolymer (poly(ethylene oxide)-poly(propylene oxide)-poly(ethylene oxide)) that is uncharged but contains several dipoles due to etheric bonds. [50] In such case only Li^+ was found to bind the polymer.

The above reported studies indicate an affinity for dipolar and carboxylate side chains that is quite low (and mutually close) for the chaotropic cations (Cs^+, Rb^+, K^+) and very strong for lithium with the Na^+ somehow between such extremes.

Such an affinity scale rationalizes the evidence that the inner charge distribution of $P^+Q_A^-Q_B$ and $P^+Q_AQ_B^-$ in CsCl, RbCl and KCl are the same but are radically different from that found for LiCl solutions if we assume that lithium ion binds efficiently to the RC. The presence of bound Li^+ changes the constellation of charges within the RC also because it likely impacts the protonation state of some acidic residues.

It should be noticed that while specific (Hofmeister) ion effects are ubiquitous phenomena, the effects of anions are, usually, stronger than those of cations and this is plausibly the reason that left the cationic Hofmeister's series less investigated. Of course specific roles of some divalent cations such as Ca^{++} and Mg^{++} in enzymatic catalysis and Cd^{++} and Zn^{++} on the $Q_A^- \rightarrow Q_B^-$ ET within the RC [51,52] are well known but a ion-specificity along the alkali cations was seldom reported.

5. Conclusions

We have demonstrated that the solution ionic strength strongly influences the rate of the ET between donor and acceptor buried within the RC. This holds both for the ET from Q_A^- to P^+ and for the ET from $P^+Q_A^-Q_B$ to $P^+Q_AQ_B^-$.

Notably both the reagents and the products of these reactions are overall electroneutral. The impact of the external ionic atmosphere on the monomolecular ET between cofactors within the protein can be understood as a consequence of the long range nature of the Coulomb interactions that are determined also by the nature of the medium surrounding the charges and not only between them [53]. Accordingly, exploiting suitable thermodynamic cycles, we have accounted for the experimental evidences considering the effect of ionic strength on the chemical potential of RC thought as a neutral protein with an internal distribution of charges.

In doing this, the protein electrostatics was described according to the lowest level of complexity sufficient to understand the impact of the ionic strength on the electrical multipoles. Strikingly, such a "spherical cow in vacuum" approach was enough to describe the observed phenomenology and to understand the electrostatic coupling between the protein multipoles and ionic atmosphere.

In the case of the thermodynamic equilibrium between $P^+Q_A^-Q_B$ and $P^+Q_AQ_B^-$, both dipole moment and quadrupole moments of the RC must be considered to reproduce the experimental behaviour.

In the case of $P^+Q_A^-$ charge recombination, the leading term was the electrical dipole moment and the salt-dependent free energy of reaction has been inserted into the classical Marcus equation for the ET rate. Such rationalizations successfully explains the experimental results.

In principle, the thermodynamic treatment can be performed exploiting the extraordinary progress made during the last decades in the explicit modeling of the electrostatic effects in the proteins. Such

an approach will surely furnish deeper insights in the ions-RC relationships in a more punctual way starting, however, from the evidences acquired to a broader level.

On an experimental ground, this study has demonstrated that it is possible to tune the ET driving force simply by changing the salt concentration also in the case of intra-protein ET monomolecular processes. Such an approach is an appealing alternative to the customary strategies used to study the intra-protein ET reactions that require the modification of the protein sequence (by mutagenesis) or the chemical modification of the cofactor in order to change the free energy gap.

Transparency document

The Transparency document associated with this article can be found, in online version.

Acknowledgments

The Center for Colloids and Surface Science (CSGI-Italy) is acknowledged for partial financial support of this work.

Appendix A. Supplementary data

Supporting Information. Details on Fluorescence measurements, recall of the Kirkwood's model, Fit of $\Delta_{AB}G°$ versus κ with three adjustable parameter. This material is available free of charge via the Internet at http://pubs.acs.org. Supplementary data associated with this article can be found in the online version, at http://dx.doi.org/10.1016/j.bbabio.2016.06.003.

References

[1] J. Israelachvili, Intermolecular and Surface Forces, Academic Press, London, UK, 1992 (chpt.14).
[2] F. Evans, H. Wennestrom, The Colloidal Domain: Where Physics, Chemistry, Biology, and Technology Meet, second ed. Wiley-VCH, 1999 (chpt. 3).
[3] G. Schreiber, G. Haran, H.X. Zhou, Chem. Rev. 109 (2009) 839–860, http://dx.doi.org/10.1021/cr800373w.
[4] W. Johan, F. Van Leeuwen, J.M. MOFERS, E.C.I. VEERMAN, Biochim. Biophys. Acta 635 (1981) 434–439, http://dx.doi.org/10.1016/0005-2728(81)90041-4.
[5] J.W. Van Leeuwen, Biochim. Biophys. Acta 743 (1983) 408–421, http://dx.doi.org/10.1016/0167-4838(83)90400-4.
[6] J.A. Watkins, M.A. Cusanovich, T.E. Meyer, G. Tollin, Protein Sci. 3 (1994) 2104–2114, http://dx.doi.org/10.1002/pro.5560031124.
[7] S. Wherland, H.B. Gray, PNAS 73 (1976) 2950–2954.
[8] D.W. Dixon, X. Hang, S.E. Woehler, A.G. Mauk, P. Bhavini, J. Sishta, Am. Chem. Soc. 112 (1990) 1082–1088.
[9] S. Guner, A. Willie, F. Millett, M.S. Caffrey, M.A. Cusanovich, D.E. Robertson, D.B. Knaff, Biochemistry 32 (1993) 4793–4800.
[10] J.T. Hazzard, S. Rong, G. Tollin, Biochemistry 30 (1991) 213–222.
[11] K. Olesen, M. Ejdeback, M.M. Crnogorac, N.M. Kostic, O. Hansson, Biochemistry 38 (1999) 16695–16705, http://dx.doi.org/10.1021/bi991242i.
[12] J.D. Rush, F. Levine, W.H. Koppenol, Biochemistry 27 (1988) 5876–5884.
[13] C.C. Moser, P.L. Dutton, Biochemistry 27 (1988) 2450–2461.
[14] E.C. Abresch, X.M. Gong, M.L. Paddock, M.Y. Okamura, Biochemistry 48 (2009) 11390–11398, http://dx.doi.org/10.1021/bi901332t.
[15] J. Deisenhofer, J.R. Norris, The Photosynthetic Reaction Center, Vol. I and II, Academic Press, San Diego, 1993.
[16] G. Feher, J.P. Allen, M.Y. Okamura, D.C. Rees, Nature 33 (1989) 111–116.
[17] C.C. Moser, C.C. Page, P.L. Dutton, Electron Transfer in Chemistry, Wiley-VCH Verlag GmbH, Weinheim, Germany, 2001 (chpt 34).
[18] C.A. Wraight, Front. Biosci. 9 (2004) 309–337.
[19] L. Kalman, P. Maroti, Biochemistry 36 (1997) 15269–15276, http://dx.doi.org/10.1021/bi971882q.
[20] K. Turzo, G. Laczko, P. Maroti, Photosynth. Res. 55 (1998) 235–240.
[21] P. Maroti, C.A. Wraight, Biophys. J. 73 (1997) 367–381, http://dx.doi.org/10.1016/S0006-3495(97)78077-9.
[22] G. Palazzo, A. Mallardi, A. Hochkoeppler, L. Cordone, G. Venturoli, Biophys. J. 82 (2002) 558–568, http://dx.doi.org/10.1016/S0006-3495(02)75421-0.
[23] F. Francia, G. Palazzo, A. Mallardi, L. Cordone, G. Venturoli, Biophys. J. 85 (2003) 2760–2775.
[24] F. Francia, M. Dezi, A. Mallardi, G. Palazzo, L. Cordone, G.J. Venturoli, Am. Chem. Soc. 130 (2008) 10240–10246, http://dx.doi.org/10.1021/ja801801p.
[25] A. Savitsky, M. Malferrari, F. Francia, G. Venturoli, K.J. Möbius, Phys. Chem. B 114 (2010) 12729–12743, http://dx.doi.org/10.1021/jp105801q.
[26] M. Malferrari, F. Francia, G.J. Venturoli, Phys. Chem. B 119 (2015) 13600–13618, http://dx.doi.org/10.1021/acs.jpcb.5b02986.
[27] S.S. Deshmukh, H. Akhavein, J.C. Williams, J.P. Allen, L. Kalman, Biochemistry 50 (2011) 5249–5262, http://dx.doi.org/10.1021/bi200595z.
[28] G. Palazzo, F. Francia, A. Mallardi, M. Giustini, F. Lopez, G.J. Venturoli, Am. Chem. Soc. 130 (2008) 9353–9363, http://dx.doi.org/10.1021/ja801963a.
[29] P. Jungwirth, P.S. Cremer, Nat. Chem. 6 (2014) 261–263, http://dx.doi.org/10.1038/nchem.1899 and references therein.
[30] A. Salis, B.W. Ninham, Chem. Soc. Rev. 43 (2014) 7358–7377, http://dx.doi.org/10.1039/c4cs00144c and references therein.
[31] W. Kunz, J. Henle, B.W. Ninham, Curr. Opin. Colloid Interface Sci. 9 (2004) 19–37, http://dx.doi.org/10.1016/j.cocis.2004.05.005.
[32] K.A. Gray, J. Wachtveitl, J. Breton, D. Oesterhelt, EMBO J. 9 (1990) 2061–2070.
[33] M. Giustini, F. Castelli, I. Husu, M. Giomini, A. Mallardi, G. Palazzo, J. Phys. Chem. B 109 (2005) 21187–21196, http://dx.doi.org/10.1021/jp054104d.
[34] M. Giustini, C. Bellinazzo, L. Galantini, A. Mallardi, G. Palazzo, S. Sennato, F. Bordi, K. Rissanen, Colloids Surf. A Physicochem. Eng. Asp. 413 (2012) 38–43, http://dx.doi.org/10.1016/j.colsurfa.2012.01.040.
[35] I. Husu, M. Giustini, G. Colafemmina, G. Palazzo, A. Mallardi, Photosynth. Res. 108 (2011) 133–142, http://dx.doi.org/10.1007/s11120-011-9666-9.
[36] D.N. LeBard, D.V. Matyushov, Phys. Chem. Chem. Phys. 12 (2010) 15335–15348, http://dx.doi.org/10.1039/C0CP01004A.
[37] D. Kleinfeld, M.Y. Okamura, G. Feher, Biochim. Biophys. Acta 766 (1984) 126–140.
[38] V.P. Shinkarev, C.A. Wraight, in: J. Deisenhofer, J.R. Norris (Eds.), The Photosynthetic Reaction Center, vol. 1, Academic Press, New York 1993, p. 193 (and references therein).
[39] G. Palazzo, A. Mallardi, M. Giustini, D. Berti, G. Venturoli, Biophys. J. 79 (2000) 1171–1179, http://dx.doi.org/10.1016/S0006-3495(00)76371-5.
[40] D. Kleinfeld, M.Y. Okamura, G. Feher, Biochemistry 23 (1984) 5780–5786.
[41] R.A. Marcus, Annu. Rev. Phys. Chem. 15 (1964) 155–196.
[42] M.R. Gunner, D.E. Robertson, P.L.J. Dutton, Phys. Chem. 90 (1986) 3783–3795.
[43] S.K. Chamorovsky, D.A. Cherepano, C.S. Chamorovsky, Y.A. Semenov, Biochim. Biophys. Acta 1767 (2007) 441–448, http://dx.doi.org/10.1016/j.bbabio.2007.01.008.
[44] A. Mallardi, M. Giustini, F. Lopez, M. Dezi, G. Venturoli, G. Palazzo, J. Phys. Chem. B 111 (2007) 3304–3314, http://dx.doi.org/10.1021/jp068385g.
[45] A. De Giacomo, C. Koral, G. Valenza, R. Gaudiuso, M. Dell'Aglio, Anal. Chem. 88 (2016) 5251–5257, http://dx.doi.org/10.1021/acs.analchem.6b00324.
[46] P.M. Krasilnikov, P.A. Mamonov, P.P. Knox, V.Z. Paschenko, A.B. Rubin, Biochim. Biophys. Acta 1767 (2007) 541–549, http://dx.doi.org/10.1016/j.bbabio.2007.02.024 (and references therein).
[47] M.S. Graige, G. Feher, M.Y. Okamura, Proc. Natl. Acad. Sci. U. S. A. 95 (1998) 11679–11684.
[48] K.P. Rembert, J. Paterová, J. Heyda, C. Hilty, P. Jungwirth, P.S. Cremer, J. Am. Chem. Soc. 134 (2012) 10039–10046, http://dx.doi.org/10.1021/ja301297g.
[49] J. Kherb, S.C. Flores, P.S. Cremer, J. Phys. Chem. B 116 (2012) 7389–7397, http://dx.doi.org/10.1021/jp212243c.
[50] J.C. Lutter, T. Wu, Y.J. Zhang, Phys. Chem. B 117 (2013) 10132–10141, http://dx.doi.org/10.1021/jp405709x.
[51] M.L. Paddock, M.S. Graige, G. Feher, M.Y. Okamura, Proc. Natl. Acad. Sci. U. S. A. 96 (1999) 6183–6188.
[52] L. Giachini, F. Francia, A. Mallardi, G. Palazzo, E. Carpenè, F. Boscherini, G. Venturoli, Biophys. J. 88 (2005) 2038–2046, http://dx.doi.org/10.1529/biophysj.104.050971.
[53] J. Israelachvili, Intermolecular and Surface Forces, Academic Press, London, UK, 1992 (chpt.3).